Shear-Induced Structuring Kinetics in Thermoplastic Segmented Polyurethanes Monitored by Rheological Tools

Elise Mourier, R. Fulchiron, Françoise Méchin

Shear-Induced Structuring Kinetics in Thermoplastic Segmented Polyurethanes Monitored by Rheological Tools

ÉLISE MOURIER[1], RENÉ FULCHIRON[1], FRANÇOISE MÉCHIN[2]

1. *Université de Lyon, CNRS UMR 5223, Ingénierie des Matériaux Polymères/Laboratoire des Matériaux Polymères et Biomatériaux, Université Lyon 1, F-69622 Villeurbanne, France*
2. *Université de Lyon, CNRS, UMR 5223, Ingénierie des Matériaux Polymères/Laboratoire des Matériaux Macromoléculaires, INSA Lyon, F-69621 Villeurbanne, France*

ABSTRACT: Thermoplastic segmented polyurethanes (TPUs) are an important class of thermoplastic elastomers with a two-phase microstructure arising from the thermodynamic incompatibility between hard (HSs) and soft segments. This microphase separation observed on cooling from a homogeneous state is often combined with the solidification of either or both types of segments. In this study, the structuring mechanism of two TPUs with HSs based on 4,4'-diphenylmethane diisocyanate and 1,4-butanediol was investigated from rheological measurements. Hence, in addition to the structuring temperature influence, the effect of an applied preshear flow in the melt polymer was analyzed, in particular. The results clearly show an enhancement of the solidification kinetics by the preshear. Indeed, the measured structuring time can be reduced by more than 1 decade. Rheo-optical microscopy observations coupled with a shearing hot stage corroborated these results and showed the modification of the microstructure by the shear.

KEYWORDS: microphase separation; morphology; polyurethanes; rheology; shear-induced structuring

Published in *Journal of Polymer Science Part B: Polymer Physics* **vol. 48**, 190-201 (2010)

DOI: 10.1002/polb.21888

INTRODUCTION

Thermoplastic segmented polyurethanes (TPUs) are one of the most important and versatile groups of polyurethanes (PU) products today, because they offer the mechanical performance characteristics of rubber, but can be processed as thermoplastics. This special characteristic of TPUs among other polymers and elastomers imparts excellent mechanical properties combined with high abrasion and chemical resistance and results in a wide array of applications ranging from ski boots and footwear to gaskets, hoses, and seals [1]. Therefore, because of their numerous manufacturing applications, these materials have received substantial interest.

TPUs correspond to a group of elastomeric polymers usually made of statistically alternating soft (SSs) and hard (HSs) segments. At ambient temperature, soft domains are above their glass transition temperature and provide the material with its rubber-like behavior. Hard domains are below their glass transition or melting temperature and are thought to govern permanent deformation, high modulus, and tensile strength.

The SSs are, in general, polyethers or polyesters and the HSs are formed from the extension of a diisocyanate with a low molar mass diol or diamine (polyurethane-ureas) as chain extender. SSs and HSs are most often thermodynamically incompatible. As a consequence of this immiscibility, a microphase separation can naturally arise leading to SS- and HS-rich phases with diverse morphologies. Moreover, the HSs, composed of polar monomers, can generate carbonyl to amino hydrogen bonds and thus tend to cluster or aggregate into more or less ordered hard domains [1]. Depending on the HS content, the morphology of the hard domains differs from isolated domains to interconnected domains [2–4]. Such a nanostructuring, therefore, requires the occurring of two different phenomena, which are, however, sometimes difficult to distinguish, namely microphase separation between rigid and soft domains and sometimes true crystallization of the HSs.

From previous studies, it is well known that thermodynamics, namely incompatibility between both kinds of segment, is the driving force for the microphase separation as studied by Cooper and coworkers [5–9]. Furthermore, some studies proved that kinetic factors, such as HS mobility and system viscosity, govern two-phase morphological structures [10–14]; and solidification can also be considered as another important kinetic factor controlling microphase separation [15,16]. This microphase separation is schematically represented in Figure 1.

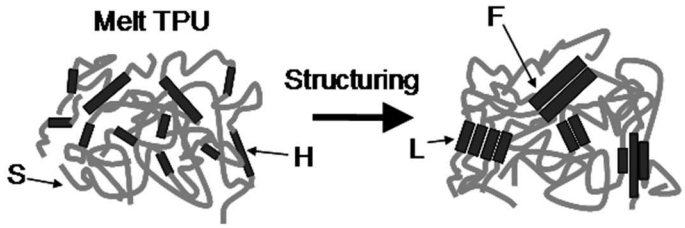

FIGURE 1. *Morphologies resulting of hard segments dispersed in the soft matrix in a thermoplastic segmented polyurethane. H, hard segments; S, soft segments; F, fibrillar domains; L, lamellar domains (inspired from ref. [17]).*

The first TPU microphase separation postulate was introduced by Cooper and Tobolsky [18]. It suggested that when the amount of SSs was high, HSs aggregated to create physically crosslinked hard domains in a soft matrix, and in the opposite, when the amount of SSs was low, phase inversion took place and SSs acted like a dispersed elastomeric phase in a rigid matrix. Koberstein and Stein's model

stated that for polyurethanes containing more than 40 wt % HSs, the shortest, with a number of repeating units below three, remained dissolved in the soft matrix unlike the longer ones, aggregated to form hard microdomains [19,20]. The average domain size of the hard phase depends on the length of the HSs, which can be adjusted through the mass fraction of diisocyanate and chain extender in the formulation and the molar mass of the polyol [21]. Previous studies showed that hard and soft domains formed a microstructure typically on a length scale of a few tens of nanometers [18,22]. Qi and Boyce revealed that these multidomain structures could evolve with deformation [23].

The final properties of TPUs depend on several parameters such as their chemical nature, thermal history, and hydrogen bonds. These variables control the arrangement, the solidification, and the final morphology [1,21,23,24–26]. Indeed, TPUs can exhibit a rich variety of transitional features, ranging from order-disorder transition (ODT), typical of block copolymers, to microphase separation and solidification [27].

Generally, TPU can be processed like thermoplastics, but it is well known that the processing of polymers generates high strain in these materials, so that the macromolecular chain orientation affects the development of the crystalline morphology. The fact that the mechanical properties of TPUs are strongly dependent on the details of the domain structure increases the complexity of the overall problem as the morphology is in turn very sensitive to the method of sample preparation. Moreover, according to Estes et al. [2], when the material is strained in the solid state, the residual orientation of different backbone segments depends strongly on strain history. Indeed, the initial strain similarly orients both segments, but after relaxation, chains containing the NH groups remain oriented to a substantially higher degree than those containing alkyl groups.

As already mentioned, TPUs can be processed like other thermoplastics via extrusion, injection molding, and so forth. However, the covalent urethane bonds in the TPU backbone are also prone to dissociate at elevated temperature. More precisely, one peculiarity of TPUs is that above their reversibility temperature, urethane bonds dissociate and reassociate simultaneously or on cooling. This phenomenon known as ‘‘transurethanization’’ can affect the HS sequence length distribution [28–30]. Also, at high temperature, the dissociation of urethane bonds causes a considerable decrease in molar mass, because the equilibrium is shifted toward the free NCO and OH end-groups [28,30–33]. Aliphatic–aliphatic urethanes are considered as the most thermally stable urethane bonds [28], whereas Camberlin et al. [34] showed that at about 200°C the urethane formation reaction from 4,4’-diphenylmethane diisocyanate (MDI) and 1,4-butanediol (BDO) became reversible. More generally, many studies in the literature show that at low or intermediate temperatures, the main degradation process of MDI-based TPUs indeed involves the splitting of urethane bonds back to isocyanates and alcohols [35], whereas using TGA the beginning of weight loss is usually observed above 250°C, in air or inert atmosphere, and whatever the nature of the SS (polyester or polyether) [36].

This thermal degradation of polyurethanes in the melt state is inevitable, because melting is usually known to occur around or beyond the stability temperature of urethane linkages. Therefore, the thermal degradation of TPU significantly affects the processing conditions and the final material properties. Lu et al. [37] explained that to understand the processing behavior and thus to predict the final properties, it was necessary to understand the rheological properties of TPU under processing conditions.

A lot of studies in the literature discuss the morphology modifications when applying a stress like annealing or stretching after the structuring of TPUs [31,38–45]. Annealing at temperatures between

Tg and Tm of the material implies a structural change of hard domains and thus increases their crystallinity. The innovative work proposed in this study is to mechanically stimulate the material in the molten state before its structuring, control the stage of nanostructuring, and eventually generate interesting nanostructures by applying a stress field giving rise, for example, to a particular anisotropy. It is well known that applying a shear before and/or during the semicrystalline polymer crystallization process enhances its kinetics and changes the resulting morphology [46–48]. Indeed, because of the shear flow, the macromolecular chain orientation promotes nucleation and then enhances crystallization.

The use of rheological techniques to investigate the phase transition behavior of polymeric systems has recently gained increasing interest [27], and many workers showed that rheology could be useful to investigate the effect of phase transition on the TPU behavior under processing conditions [49–51]. Nevertheless, Cossar et al. [27] pointed out that rheology alone was not in principle able to differentiate between phase separation and ODT, where the former is associated with a change in either the nature or the number of phases, whereas the latter is only characterized by a change in the degree of order of the system.

The aim of this study is to highlight the shear effect on the complex morphology of TPUs and to allow a better apprehending of the effects that processing can produce on the microstructure of these materials.

EXPERIMENTAL

Materials

Two commercial thermoplastic polyurethanes with different chemical structures were used for this study. Both were at first characterized by NMR (^{1}H and ^{13}C), to determine the chemical nature and average length of their SSs, together with the composition and average weight proportion of the HSs, or in other words, the urethane equivalent weight of these two TPUs. The simplified chemical structures found for these two materials are depicted in Figure 2.

Estane 58887, labeled PU1, already studied by Lapprand et al. [52] and supplied by Noveon (now Lubrizol) is based on MDI and BDO for the HSs, and on a polyether SS (polytetramethylene oxide, POTM, with a molar mass ~1000 g/mol). Depending on the signal integration used for calculation, the average number of BDO units in each HS lies between 1.6 and 1.8 (i.e., an average molar mass between 640 and 850 g/mol for the HSs). This is thus rather short, but the SS is also not very long. The observed integration values correspond to a global HS proportion of 45–46 wt %, and to a urethane equivalent weight = 335–340 $g/mol_{urethane\ bond}$.

Estane 58213, labeled PU2, also supplied by Noveon, is composed of MDI/BDO HSs and of a polyester (polybutylene adipate) SS with a molar mass ~1500 g/mol. Considering this value, calculations based on the various integrations showed that the average number of BDO unit per HS was about 0.8, that is, an average molar mass of about 520 g/mol for these HSs; in other words, NMR studies suggest that these MDI/BDO units are presumably so short that their crystallization is difficult in the case of PU2. Here, the HS proportion was 26 wt %, whereas the value for urethane equivalent weight was found equal to 565 $g/mol_{urethane\ bond}$. Therefore, PU2 has fewer urethane links and also fewer and shorter HSs

than PU1. These results already suggest that the miscibility between SSs and HSs might be higher in the case of PU2 [8], and that the ability of the hard phase of PU2 to crystallize might also be quite low, whereas in PU1, crystallization could still take place in the HS phase.

Methods

The aim of this work was to analyze how a shear treatment in the melt state can influence the solidification process of the materials. In the following, the term ‘‘solidification’’ will mean the evolution from the melt to a solid state of TPUs, this phenomenon being possibly due to crystallization or to vitrification of the rigid domains. Before each experiment, material pellets were dried in a vacuum oven at 80°C for a minimum of 4 h. Solidification under quiescent (without preshear) conditions and solidification under shear flow were followed by calorimetry, by rheological, and by rheo-optical measurements.

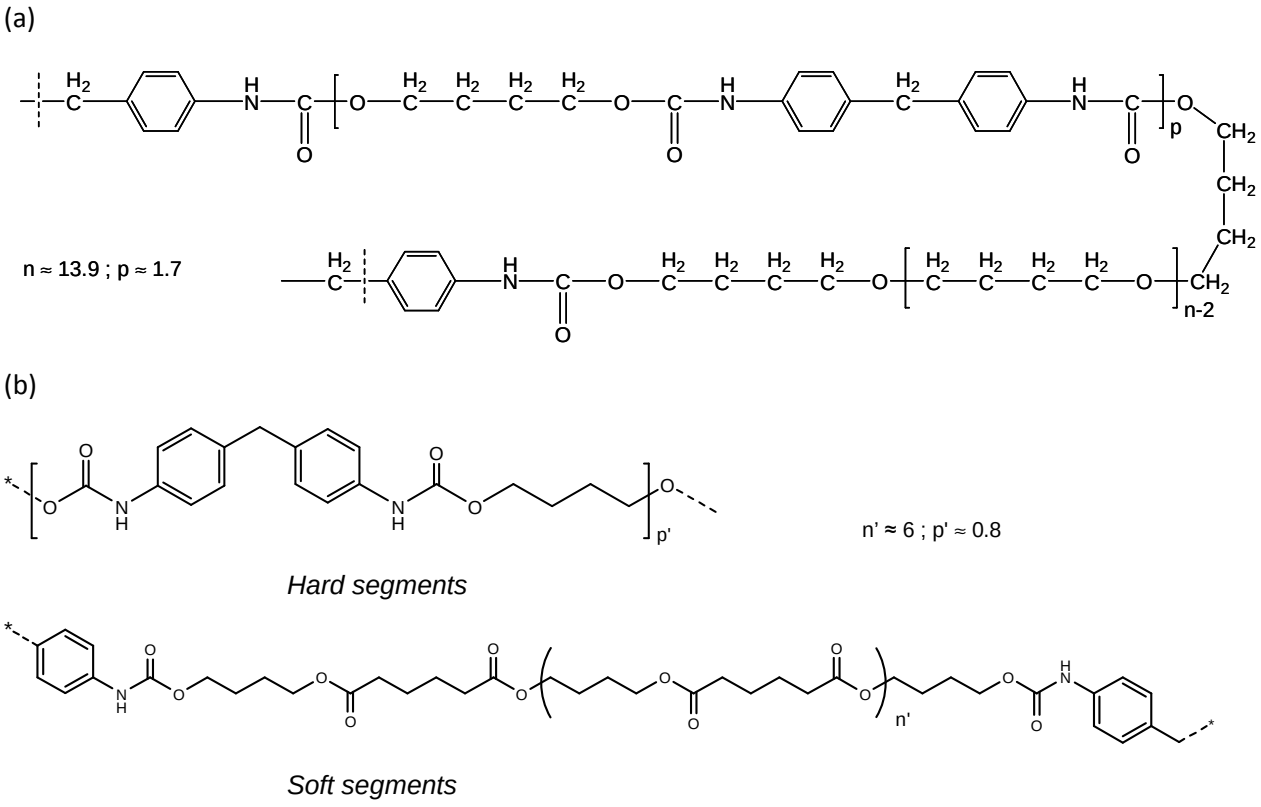

FIGURE 2. *Average chemical structure of the studied TPUs determined by ^{1}H and ^{13}C NMR. (a) PU1 and (b) PU2.*

Size Exclusion Chromatography

Size Exclusion Chromatography (SEC) experiments were performed in tetrahydrofuran (THF) at 22°C using a system equipped with a Waters 410 differential refractometer, a Waters 510 pump with a flow rate of 0.5 mL/min, a Rheodyn 7725I injector, and a PL Gel mixed C column (internal diameter 7.8 mm, length 30 cm). Absolute molecular weights were calculated owing to a Wyatt miniDAWN 3 angle multiangle light scattering instrument, and results were obtained thanks to ASTRA 5.3.4.13 software.

Calorimetry Measurements

Static solidification measurements were performed using a Pyris Diamond differential scanning calorimeter (DSC) from Perkin–Elmer calibrated with indium standard. Slices of dried pellets (between 8 and 10 mg) were placed in an aluminum pan and were molten under inert atmosphere at 220°C for PU1 and at 180°C for PU2, then held at these temperatures for 3 min to erase all previous thermal history. Then, the temperature was decreased at 10°C/min down to -60°C. The temperature of crystallization T_c was defined as the temperature of the crystallization peak minimum (see e.g., Fig. 3). Finally, the temperature was increased at 20°C/min to record the material melting temperature T_m (peak maximum).

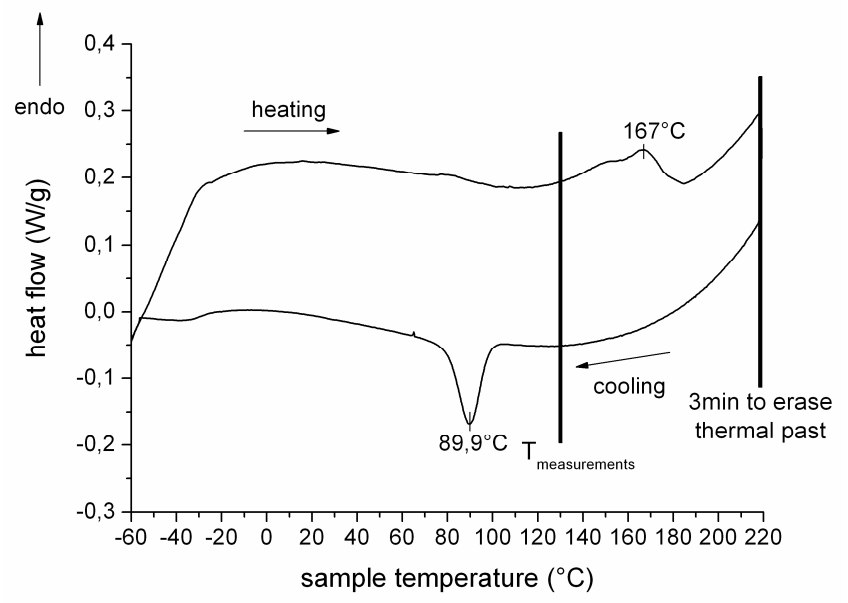

FIGURE 3. *DSC trace during a solidification experiment of PU1 at a constant cooling rate of 10°C/min followed by a heating run at 20°C/min.*

Rheological Measurements

To deeply investigate the structuring processes of the materials, different rheological measurements were performed in a strain-controlled rheometer, RMS 800, from Rheometrics Scientific. First, some temperature sweep experiments were carried out at a frequency of 1 rad/s, from the melt following the same thermal profile as for DSC measurements and using a parallel plate geometry (diameter 25 mm, gap 1 mm).

Following a methodology used for the characterization of the flow-induced crystallization kinetics for different polymers [53,54], time sweep measurements were performed. For these experiments, a cone and plate configuration was used (diameter 8 mm, cone angle 0.1 rad) to ensure the strain homogeneity in the sample, which is essential for studying the effect of the preshear. One pellet was placed in the rheometer cell and was molten under the same conditions as for calorimetry measurements. Then, it was cooled down as quick as possible to the required solidification temperature. As soon as this temperature was reached, the desired preshear treatment defined by the shear rate and the shear duration was carried out. All these preshears were applied after the same cooling time for all the samples. The sample was then kept at the same temperature, and the storage

(G') and loss (G") moduli were recorded until an equilibrium state was reached after their crossing. For this part of the experiment, the frequency and strain were set to 1 rad/s and 3%, respectively. The solidification kinetics was deduced from the evolution of the storage modulus G' and of the loss modulus G", and a characteristic time for solidification was defined as the time of the interception of both moduli. Finally, reference rheological experiments without any preshear but at different temperatures (110–150°C for PU1; 60–80°C for PU2) were performed following this procedure of time sweep analyses.

Rheo-Optic Measurements

Quiescent and shear-induced solidification experiments were carried out in the shearing hot stage CSS 450 from Linkam Scientific Instruments (UK) coupled with an optical microscope Orthoplan from Leitz. Pellets of material were placed in the hot stage and the gap was set to 250 µm after the sample melting. Following the same procedure as for rheological measurements, samples were molten at 220°C for PU1 and 180°C for PU2 for 3 min and then cooled to the desired solidification temperature at the maximum available cooling rate (30°C/min). Experiments were carried out at 135°C for PU1 and 80°C for PU2 to approach the conditions of the rheological experiments for both materials. As soon as the solidification temperature was reached, the shearing step defined by a shear rate and a shearing time was applied and data collection (pictures and light intensity) started. In these cases, crossed polarizers were used to analyze the solidification by optical microscopy. Under such conditions, the transmitted light intensity increases during crystallization, in the case of semicrystalline materials, because of the crystallite birefringence.

RESULTS AND DISCUSSION

Preliminary Studies on the Thermal Stability of the TPUs

Here, all the described rheological and thermal experiments were performed in nitrogen atmosphere to limit the degradation, and at a maximum temperature of 200°C (except, for PU1, the very short initial thermal treatment at 220°C to erase thermal history). Moreover, not only for the rheological experiments but also for the microscopic ones, the sample is so confined that the surface directly in contact with the atmosphere is negligible. Furthermore, the applied thermal treatments for the described experiments are surely less severe than what is undergone by the material during its processing. However, in the case of PU1, as already underlined by Lapprand et al. [52], the molar mass of materials was indeed affected by an applied thermal treatment used to erase thermal history. SEC measurements were therefore performed in THF to verify the effect on sample molar mass of the thermal treatments applied before or during several experiments proposed in this study. Samples were, thus, subjected to analogous temperature cycles, then either quenched or slowly cooled, and then immediately dissolved. A mixture of THF and di-n-butylamine (2.5 vol %) was used for that purpose. In so doing, the secondary amine was expected to neutralize the free isocyanates, to prevent any further recombination and, therefore, to have an exact image of the real, original molar mass distribution at high temperature in the case of quenched samples. The sample concentration was about 2 g/L. Results are summed up in Table 1.

TABLE 1. *Molar Masses of Initial Pellets and Thermally Treated Samples*

		Quenched samples		Slowly cooled samples	
PU1	Reference	After 3 min at 220°C	After 3 min at 220°C + 40 min at 200°C	After 3 min at 220°C	After 3 min at 220°C + 40 min at 200°C
M_w (g/mol)	96,800	53,900	64,500	62,200	79,200
		Quenched samples		Slowly cooled samples	
PU2	Reference	After 3 min at 180°C	After 3 + 40 min at 200°C	After 3 + 40 min at 200°C	
M_w (g/mol)	67,600	71,100	57,000	63,600	

For PU1, after 3 min at elevated temperature, the sample molar mass is half lower than the reference one, but some chain reorganizations together with a molar mass increase were allowed for a slowly cooled sample. Annealing for 40 min at intermediate temperature (200°C) allowed even more mass recovery. This is in good agreement with the literature. For example, Hentschel and Münstedt [55] proved that the decrease in molar mass could be entirely reversible, if no other side reactions are possible (inert atmosphere) and if the cooling is slow enough to leave sufficient mobility for the created reactive groups to be able to recombine.

At high temperature, other side reactions such as crosslinking were occasionally mentioned in the literature [56] for example, during the extrusion of a medical-grade polyether-based TPU, but only above 210°C during processing; whereas during rheological experiments on this same TPU, a strong oxidative crosslinking was evidenced in air at 240°C, but the same phenomenon was shown to become negligible at 180°C in air and even at 200°C in an inert atmosphere. Therefore, in our opinion, such type of degradation under our experimental conditions is rather unlikely; moreover, the samples used for the SEC analyses seemed perfectly soluble, and the areas of the peaks associated with the analyzed fractions rather constant.

Temperatures used for PU2 being lower than for PU1, the molar mass of PU2 was consequently less affected by the applied thermal treatments. In any case, in this work, the possible thermal degradation of hard domains was always considered for the following discussions.

Solidification in Cooling Mode

As preliminary experiments, the solidification from the melt state was followed using both DSC and rheological measurements with controlled cooling rate. For PU1, DSC traces presented in Figure 3 confirm a crystallization temperature around 90°C for a cooling rate of 10°C/min. This temperature is close to the G' and G" crossing temperature in the temperature sweep experiment (96°C) for the same cooling rate, shown in Figure 4. This can prove that, in this case, the G' and G" crossover can be mainly attributed to the solidification of the HSs, that is their crystallization. Note that no special phenomenon that could be associated with microphase separation is visible in this thermogram. Then in the following heating scan, the measured melting temperature was around 170°C. However, no glass transition was detected but this does not necessarily indicate that it does not exist. Indeed, Camberlin et al. [34] showed that if any glass transition occurs, the heat capacity variation can be very weak in the case of HSs based on MDI/BDO, and the detection by DSC can also be difficult, if the glass transition occurs over a wide range of temperatures in the case of a broad molar mass distribution for the HSs.

Contrary to PU1, no crystallization or melting peak was clearly distinguished on the DSC trace of PU2, shown in Figure 5, in agreement with the fact that in PU2, the amount of HSs is lower and these HSs are likely too short to easily crystallize. However, it can be pointed out that an event is detected around 120°C in the heating run, which is a very weak and broad endothermic peak. If this peak could be ascribed to a possible crystallinity, it is anyway very small. Besides, a glass transition can clearly be observed around -30°C, which likely corresponds to the polyadipate SSs mixed with some dissolved HSs. The T_g of the starting polyadipate SSs (M_w 1500 g/mol) indeed lies around -70°C [57]. Even after polycondensation, this value cannot be increased by more than 10–15°C, and therefore, the presence of dissolved HSs in the soft phase must be invoked to account for this high value [58], consistently with their short length.

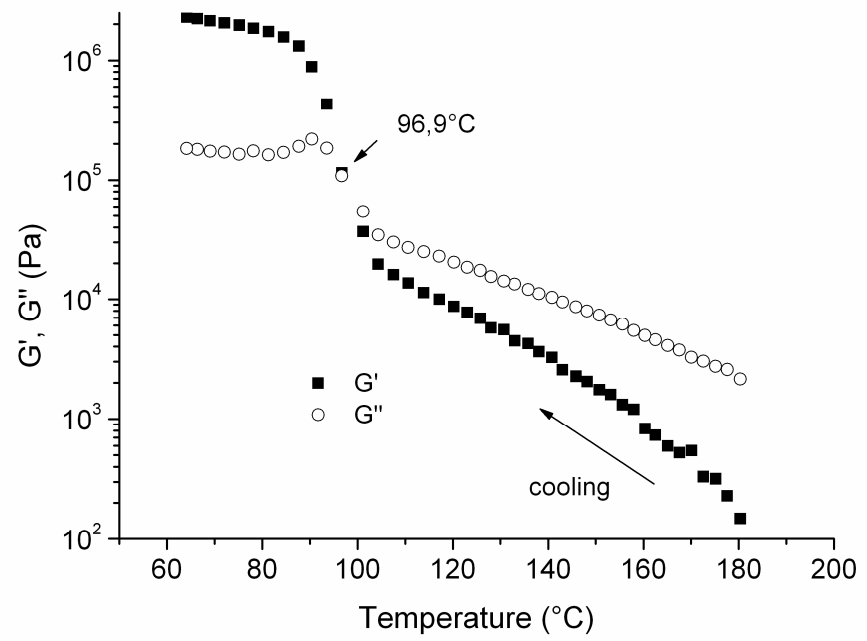

FIGURE 4. *Temperature sweep experiment on PU1 at a constant cooling rate of 10°C/min.*

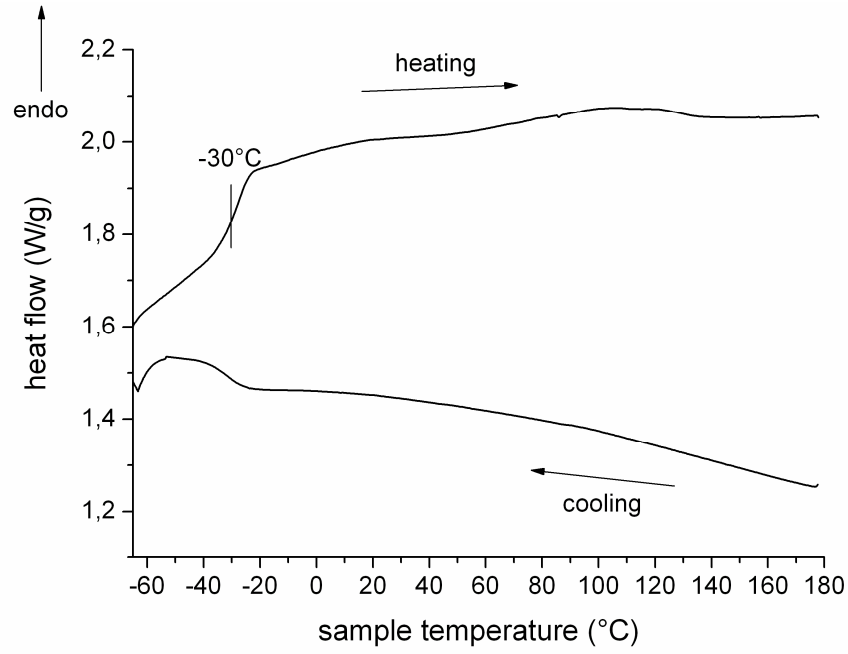

FIGURE 5. *DSC trace during a cooling experiment of PU2 at a constant cooling rate of 10°C/min followed by a heating run at 20°C/min.*

For the rheological measurement presented in Figure 6, the G' and G" moduli crossing occurs at around 51°C, which is almost the lower limit of the rheometer thermal regulation. Here again, the G'/G" crossing is correlated to the structuring process of the material. However, according to the DSC measurements, it is not obvious to attribute this structuring to a real crystallization, but rather the vitrification of some HS-rich domains that would then act as physical crosslinks could be invoked. In any case, this experiment shows that in this case of short HSs, the structuring on cooling occurs at a

lower temperature. This could also denote a higher solubility of these short HSs. As already noted by Nichetti and Grizzuti in the literature [24], DSC is less sensitive to the microstructural morphological changes taking place in the TPUs than rheological measurements. Indeed, in this case of a practically amorphous TPU, no structural change was noticed in the cooling run of the DSC experiment around 50°C.

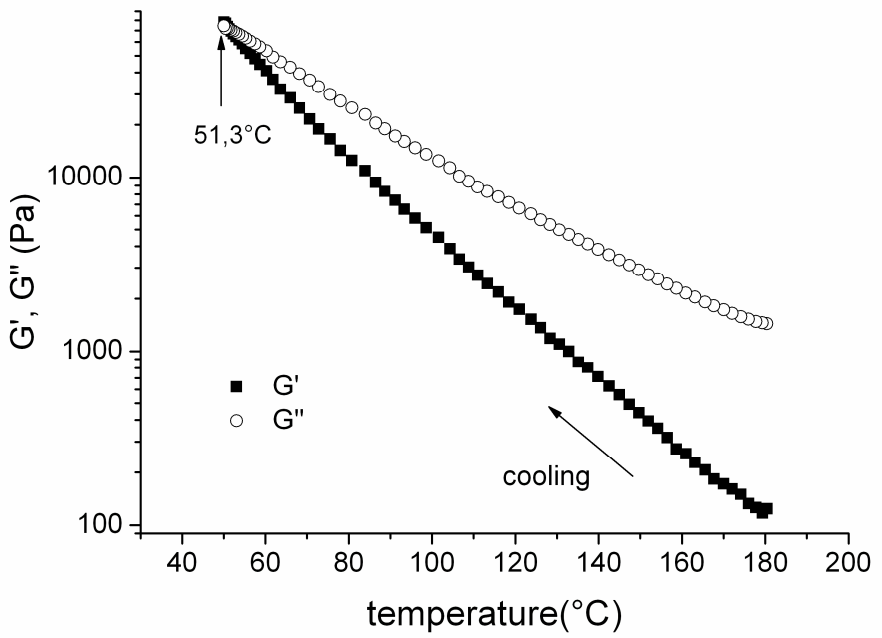

FIGURE 6. *Temperature sweep experiment on PU2 at a constant cooling rate of 10°C/min.*

Furthermore, these experiments allowed us to determine the temperature protocol applied before each experiment for all the further isothermal measurements. The measurement temperature has to be higher than all the obtained solidification temperatures. The temperature reached to erase thermal past has to be above all the melting transitions. Therefore, the temperatures of 130°C for PU1 and 80°C for PU2 were chosen for the solidification experiments after shear flow followed by rheology, which will be discussed later.

Static Microphase Separation and Solidification in Isothermal Conditions

The structuring mechanism without any preshear was first analyzed from time sweep rheological experiments, as described in the Experimental section. These experiments were carried out at several temperatures, ranging between solidification and melting temperatures for the semicrystalline sample (PU1) and in any case above all glass transition temperatures for both samples. More precisely, the experiments were run between 110 and 150°C for PU1 and between 60 and 80°C for PU2. In both cases, no special thermal degradation is therefore expected for the studied TPU in the considered temperature range, but some mass recovery could occur during the experiment, to an extent comparable with what was observed in the ‘‘quenched sample + 40 min isotherm’’ experiments described in Table 1. At the beginning of this isothermal time sweep experiment, the TPU is indeed entirely fluid and homogeneous (i.e., with enough mobility), but at a temperature low enough to allow isocyanate/alcohol recombination and moreover, there is almost no atmosphere except on the edges where only nitrogen is present. The results for PU1 are shown in Figure 7.

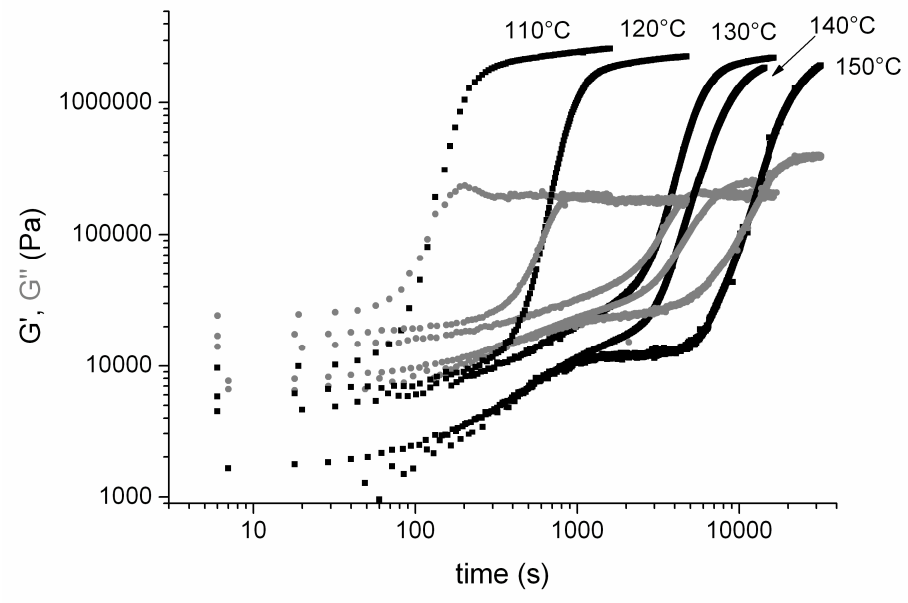

FIGURE 7. *Time sweep experiments for PU1 at different temperatures.*

For every temperature, the curve evolution can be described as follows: when the desired temperature is reached, G' first slightly increases, but remains lower than G" during a definite time where the global behavior of the material remains liquid. This first slow increase is due to the slight molar mass increase, discussed just earlier. For that part of the curves, the initial value of G' decreases upon increasing temperature, which is typical of a melt polymer behavior. Moreover, during this period and especially, for the highest temperatures (140 and 150°C), after the small increase, G' exhibits a plateau at about 2 X 10^4 Pa. The beginning of this plateau corresponds to the achievement of the molar mass recovery. Then, at intermediate times, G' and G" sharply increase and cross each other. In the following, this crossover time will be considered as characteristic of the structuring time. From these results, it is obvious that the structuring kinetics is lowered when the temperature increases. Finally, for longer times, the G' and G" evolutions become smooth again, after a slight overshoot for G". It can be noticed that Nichetti and Grizzuti [24] observed that no final equilibrium state was ever reached, even after many hours of isotherm, more than 1 day. In our case, the experiments were not prolonged during such long times but nevertheless, it seems that the equilibrium state is not obtained either. This response of the dynamic modulus during the isothermal treatment of the TPU corresponds to the behavior already described in the literature by Cossar et al. [27] and is typical of systems undergoing a transition from a liquid-like to a solidlike behavior. Such a transition is characterized by the passage through a critical gel state. This gel behavior is likely due to the formation and growth of HS ordered/crystalline aggregates, which act as reticulation nodes. Indeed, according to Rek and Govorcin [59], during the annealing period, the mobile HSs appear to reassociate into more stable hard domains and then create better ordered hard domains with increased crystallinity. The critical gel point is then reached when such aggregates become sufficiently interconnected, thus generating a relatively hard gel. In this study, we consider that the crossover of these two moduli can correspond to the critical physical gel (network) point in the studied polyurethanes.

As shown in Figure 8, for PU2 where the HSs are shorter, the experiment temperature has to be decreased down to 70°C to achieve a G' and G" crossover within 10,000 s. However, again, the initial measured G' is higher for lower temperature reflecting the thermal behavior of a liquid polymer.

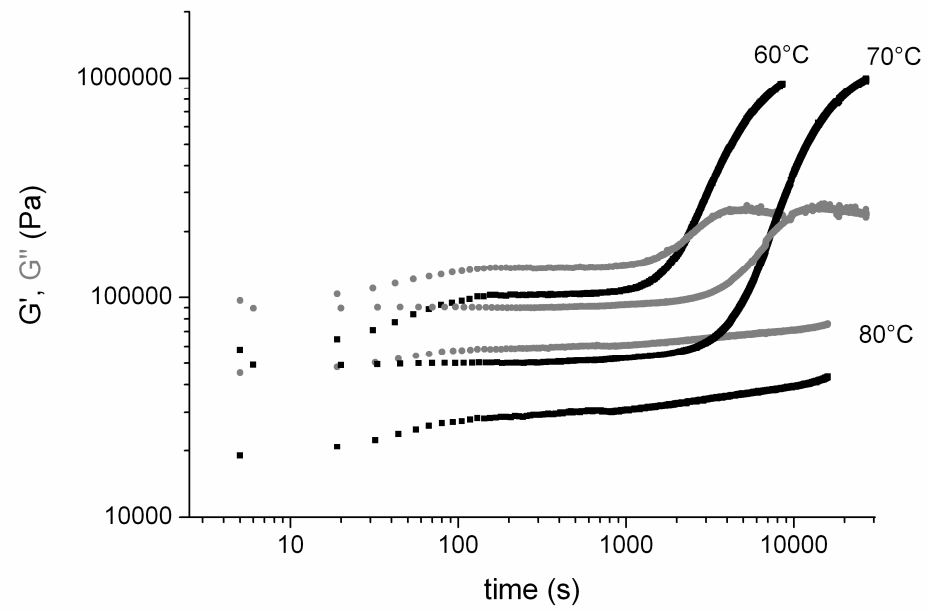

FIGURE 8. *Time sweep experiments for PU2 at different temperatures.*

Effect of a Preshear Treatment on the Solidification

As previously mentioned, for both studied polyurethanes, the temperature of the isothermal experiments was determined from the previous DSC results, in the range of solidification and melting temperatures for PU1 and above the glass transition temperature for PU2. Time sweep tests with a preshear treatment were then performed, as described in the Experimental section.

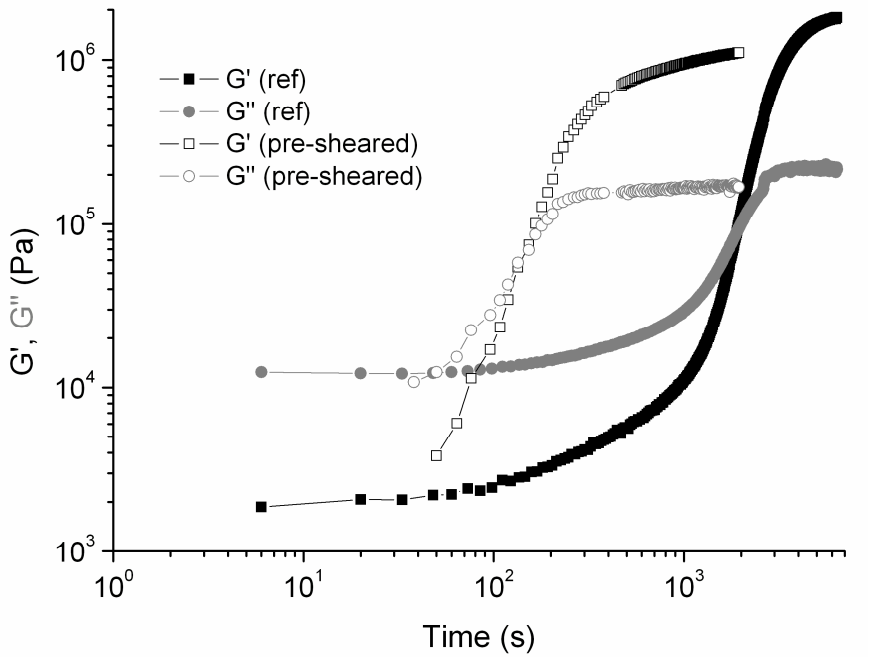

FIGURE 9. *Moduli G', G" evolution during a time sweep experiment at 130°C for PU1 with or without preshear. The applied preshear was 10 s^{-1} during 30 s.*

As an example, the dynamic modulus for PU1 is reported in Figure 9 for two experiments, one without preshear (‘‘reference sample’’) and the other with a preshear of 10 s^{-1} during 30 s. The enhancement of the structuring (crystallization and/or microphase separation) kinetics is clearly observed for the presheared sample. Indeed, the G’ and G” crossing time appears more than 1 decade lower for the presheared sample.

Similar experiments were performed with applying several shearing conditions. The results are summed up in Figure 10, where the moduli crossing times were reported versus the applied shear rate, for various preshearing times. These results reflect the general trend, which is a large decrease in the structuring time, up to 1 decade for a shear rate of only 5 s^{-1}. Furthermore, the longer is the preshear time, the lower is the structuring time.

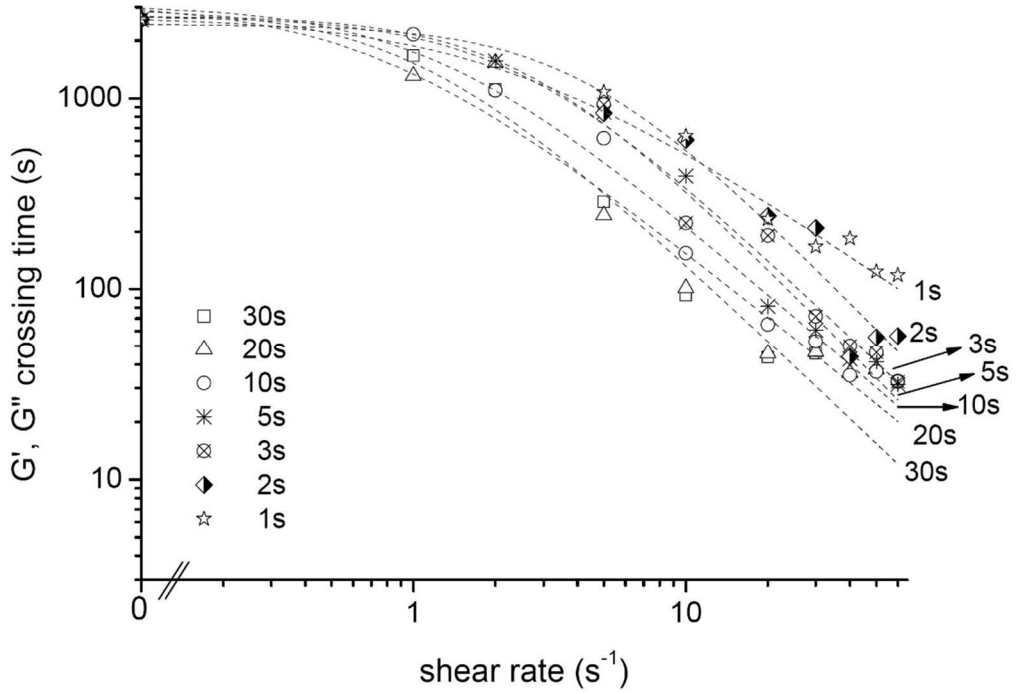

FIGURE 10. *Moduli G’, G” crossover time variation as a function of the applied shear rate at 130°C and of its duration (see legend), for PU1 (dash lines stand only as eye guides through the experimental data).*

Moreover, the temperature effect on the shear-induced structuring was investigated and the main results are shown in Figure 11, where the moduli crossing times are reported for experiments with and without a preshear treatment. Following Cossar et al. [27], the temperature effect can be empirically fitted using an Arrhenius equation. Equations 1–3 give the obtained numerical results for nonpresheared and presheared samples:

$$t_{cross}[s] = 1.83 \times 10^{25} exp\left(\frac{-20400}{T}\right) \quad (1)$$

without preshear,

$$t_{cross}[s] = 4.39 \times 10^{22} exp\left(\frac{-18500}{T}\right) \quad (2)$$

for a preshear of 10 s^{-1} during 5 s and

$$t_{cross}[s] = 1.49 \times 10^{13} exp\left(\frac{-10600}{T}\right) \quad (3)$$

for a preshear of 30 s^{-1} during 5 s.

At this stage, some comments can be introduced concerning the solidification mechanism whose kinetics should be governed by the slowest phenomenon between microphase separation and crystallization. However, it is far from obvious to determine which one is the slowest. Nevertheless, in both cases, the global trend of the plot of the solidification characteristic times versus the temperature should lie on a U-shaped curve (or a bell-shaped curve in terms of solidification velocity). Indeed, for relatively high temperatures, the phase separation mechanism kinetics for block copolymers (melts or solutions) is mainly governed by the so-called quenching depth, which is evaluated by the difference between the temperature of the order–disorder transition (T_{ODT}) and the actual temperature [60–62]. For the crystallization mechanism, still in the high temperature range, the kinetics is also governed by a temperature difference, namely the supercooling, which is the difference between the melting temperature of the infinite crystal (T^0_m) and the actual temperature [63]. Anyways, for this high temperature range, the solidification time decreases when the considered temperature difference increases, that is, when the actual temperature decreases. Nevertheless, this trend should not follow an Arrhenius law. Conversely, in the lower temperature range, both mechanisms (phase separation and crystallization) are governed by the diffusion of molecules and therefore can follow an Arrhenius law [62]. Obviously, in that case, the solidification time increases when the temperature decreases.

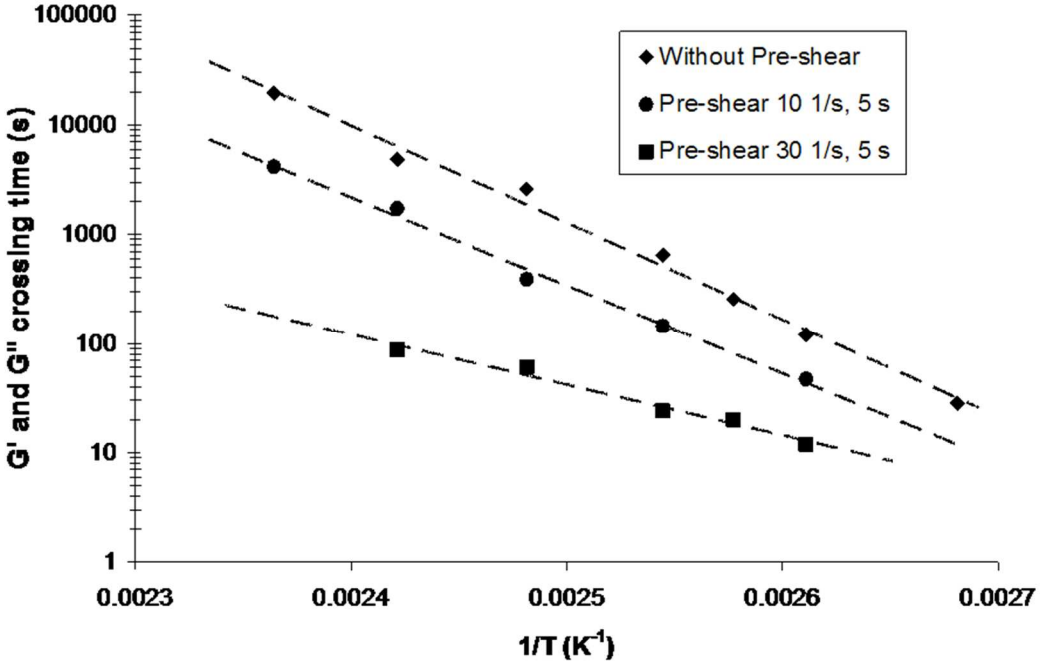

FIGURE 11. *G' and G" crossing times for PU1 as a function of the reciprocal temperature with and without preshear.*

Thus, as concerns the results shown in Figure 11, as the obtained solidification time decreases when the temperatures decreases, it follows that the investigated temperature range corresponds to a mechanism, which is not controlled by the molecular diffusion capability but rather by the driving force resulting from the difference between the equilibrium state (defined by T_{ODT} or T^0_m) and the actual state given by the temperature T. Thus, the surprisingly obtained Arrhenius laws can only be considered empirical. However, the linearity of the plots in Figure 11 must be pointed out. Moreover,

from these results, it must be added that this thermodynamically governed mechanism is indubitably enhanced by a preshear treatment as it was already shown for phase separation of polymer blends [64] and for polymer crystallization [39–41].

At this stage, it should have been relevant to introduce an evaluation of the mean relaxation time (λ) of the material at the solidification temperature. Indeed, by analogy with what is generally acknowledged for the flow-induced crystallization [53], the comparison of the shear rate and this relaxation time via the Weissenberg ($W_e = \lambda\dot{\gamma}$) should provide a suitable criterion to predict whether the structuring process will be sensitive to the shear or not. Unfortunately, a proper determination of the relaxation time was not possible with the studied material, mainly because of the previously described molar mass change at high temperature. Indeed, the relaxation time value at the structuring temperature must be extrapolated from higher temperatures on the basis of the time-temperature superposition principle applied on several linear viscoelastic experiments. However, this principle is applicable only if the material molecular structure is not affected by the temperature. Nevertheless, for the studied TPU (especially PU1), the molecular weight evolves along the time at high temperatures as it was shown earlier. Thus, only a very rough order-of-magnitude estimate of the relaxation time can be attempted. Therefore, frequency sweep experiments (not shown in this article) were performed, and the estimated relaxation time was ~0.5 s. This value is not in contradiction with the critical shear rate marking the difference between the two observed microstructure evolution mechanisms in Figure 10 (~2–5 s^{-1} leading to W_e ~ 1).

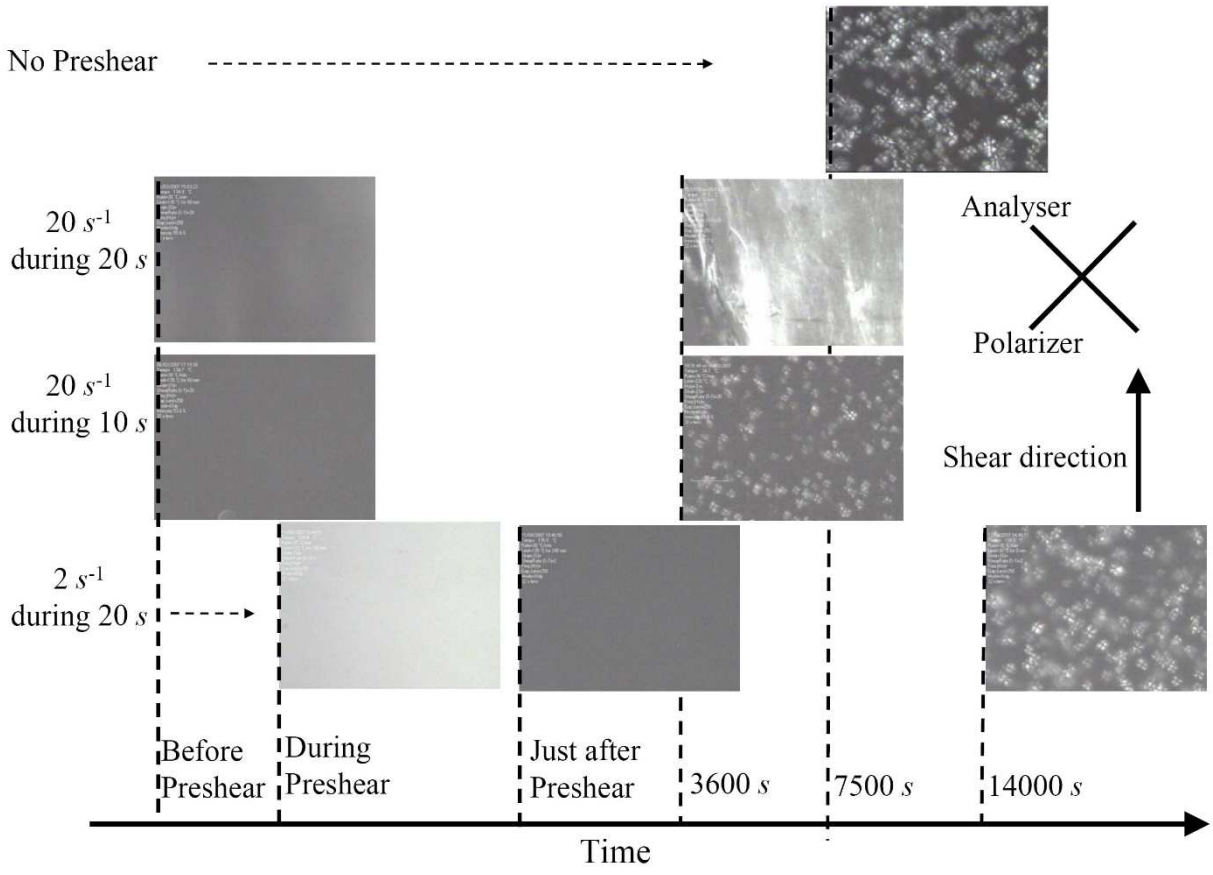

FIGURE 12. *Micrographs of PU1 versus time obtained at 135°C for different shear treatments (indicated in the left part). The height of a picture corresponds to 400 µm.*

Rheo-optical measurements were performed to simply analyze the evolution of the morphology of the TPU during the structuring and possible crystallization of the polyurethane. For PU1, all the results obtained at 135°C are gathered in Figures 12 and 13. In Figure 12, micrographs drawn from four experiments with different preshear treatments are shown versus a time scale. In Figure 13, the transmitted light intensity is shown for experiments with (b and c) and without (a) preshear. Without any preshear, the final morphology of PU1 reveals some spherulites of around 20 µm diameter. Simultaneously, the transmitted light intensity slowly increases during more than 7000 s to finally achieve a constant value. The time corresponding to the half intensity variation is around 2700 s (~45 min), which is similar to the moduli crossing time during rheological time sweep experiment for a reference sample (~2600 s).

Concerning the effect of deformation, different results can be observed depending on the preshear conditions in terms of shear rate or shear duration. In fact, for relatively ''soft'' preshears (20 s^{-1} for 10 s and 2 s^{-1} for 20 s), during the preshear the transmitted light intensity first increases [Fig. 13(c)] simultaneously with a global lightening in the micrograph (lower row of Fig. 12). However, no spherulites are noticeable at this stage. Indeed, the revealed birefringence is due to the molecular orientation consequently to the shear. Then, immediately after the preshear, because of molecular relaxation, the transmitted light decreases and the micrograph becomes dark again. Afterward, some spherulites appear, which are slightly smaller than without preshear, as it was already reported for semicrystalline homopolymers [46–48]. However, in these cases of moderate preshear treatments, there is no significant effect of these preshears in terms of final spherulitic morphology. Nevertheless, in terms of structuring kinetics, the effect can remain noticeable [see Fig. 13(a,b)].

For stronger preshear treatments (second row of Fig. 12), the micrographs also show some brightness during the shear, but after its cessation, this brightness remains quasi constant without the appearance of spherulites. In that case, it appears that the material structuring is achieved during the preshear, and that the molecular orientation provided by the shear is maintained after its ending. The transmitted intensity variation (not shown here) confirms this result: during the preshear it increases and exhibits a somehow chaotic variation (likely due to flow disruptions), and then, after the shear ends, it stabilizes and remains constant at a level higher than the initial one. These results prove that the sample morphology is largely dependent on the preshear conditions. Actually, according to the shearing strength, the sample morphology can be frozen during the shear (without development of spherulites) or can evolve during the isotherm (with growth of spherulites).

As for PU1, rheological tools were used to analyze the solidification behavior of PU2. Figure 14 shows the time evolution of G’ and G” for PU2 with or without preshear treatment. At 80°C, during an experiment of more than 20,000 s (~5 h 30 min), no interception between moduli ever appeared, while when a preshear was applied, once the isothermal temperature (80°C) was reached, the moduli crossed around 870 s later. This experiment confirms that when a stress is applied before material structuring, the kinetics of this phenomenon is tremendously modified.

The results for PU2 are summed up in Figure 15, where the G’ and G” crossing times are plotted versus the applied shear rate for a preshearing time of 10 s and a measurement temperature of 60°C. Indeed, at this temperature, the G’/G” crossover without preshear was obtained for a reasonable experimental time, contrary to the results at 80°C in Figure 14.

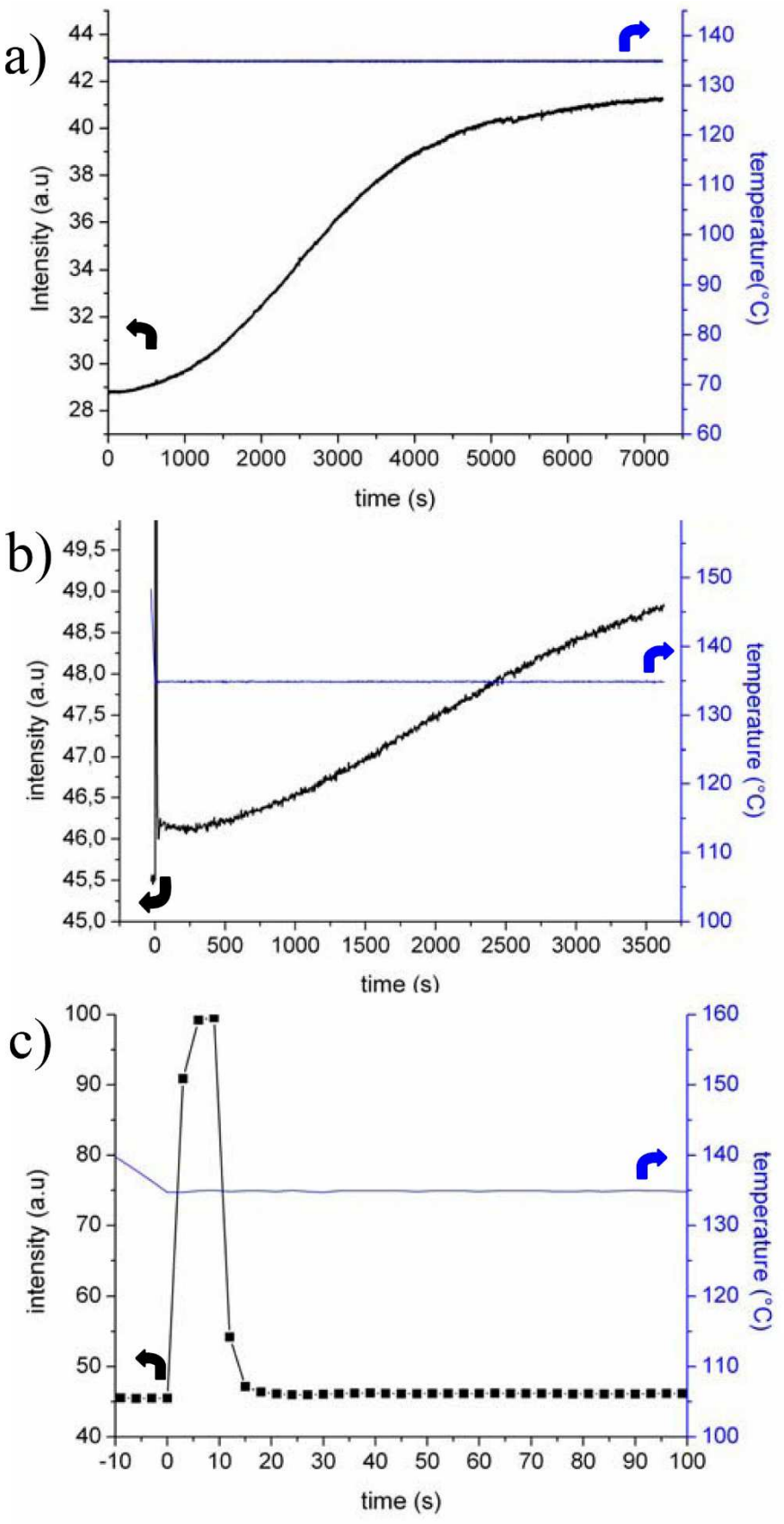

FIGURE 13. *Transmitted light intensity for PU1 during a solidification experiment at 135°C. (a) Without preshear, (b) with a preshear of 20 s^{-1} during 10 s, and (c) beginning magnification of (b).*

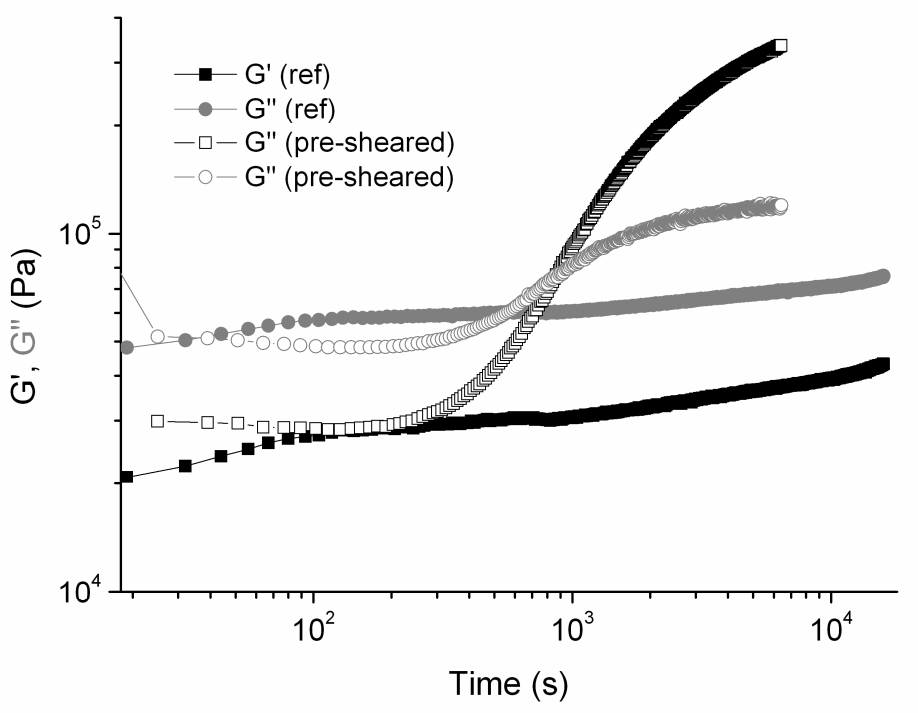

FIGURE 14. *Moduli G', G" evolution during a time sweep at 80°C for PU2 with or without preshear. The applied preshear was 40 s^{-1}/5 s.*

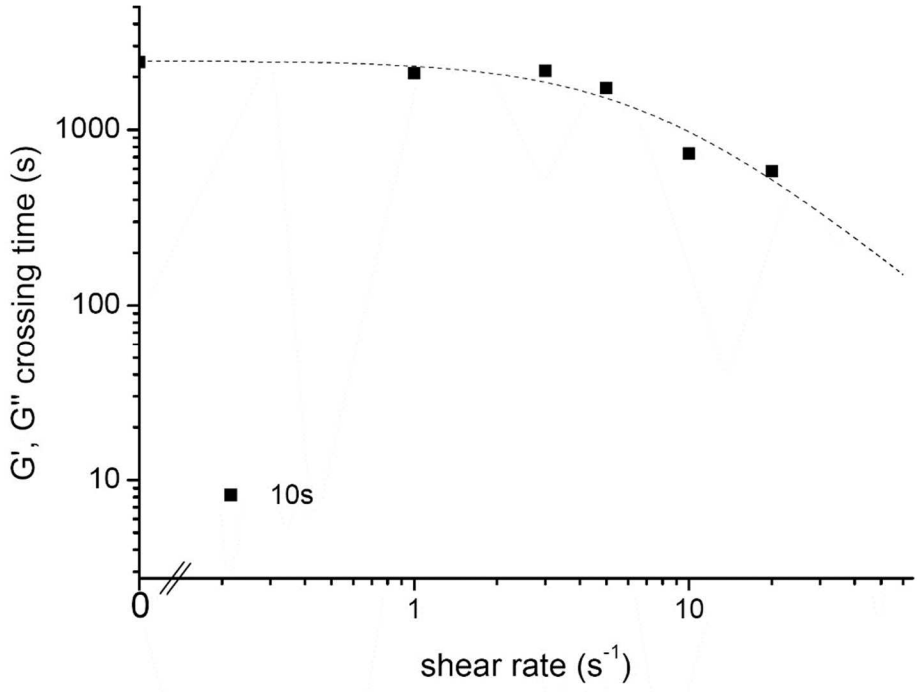

FIGURE 15. *Moduli G', G" crossover time variation as a function of the applied shear rate during 10 s at 60°C, for PU2.*

Moreover, quite similarly to what was shown for PU1 (Fig. 11), the results for PU2 could be displayed on Arrhenius plots (not shown in this paper), leading to similar apparent activation energies but with higher preexponential factors.

Rheo-optical measurements were also performed for PU2 to follow the isothermal solidification at 80°C. However, for the reference experiment without any preshear, even after 10,000 s, no crystalline entities were detected on the micrographs (not shown here) in accordance with the calorimetric studies of this polyurethane. Moreover, neither increase of the brightness nor transmitted light variation was detected.

Conversely, for experiments with substantial preshear treatments, an evolution of the transmitted light intensity was observed. During the shear, an increase in the intensity was observed, generally followed by irregular variations (similarly to the results for PU1 with strong shear treatments). Then after the shear, the intensity stabilized at a value slightly higher than the initial one. This could indicate that the morphology was frozen. Figure 16 shows successive micrographs taken during such an experiment. The birefringence of the solidified material induced by the shear is evidenced. Therefore, it can be deduced that there is an orientation of the morphology due to the preshear, but practically no evolution of the structured morphology is detected afterward. These experiments confirm that even if the material PU2 is practically amorphous, the final structure can be different depending on whether a stress is applied before or during the solidification.

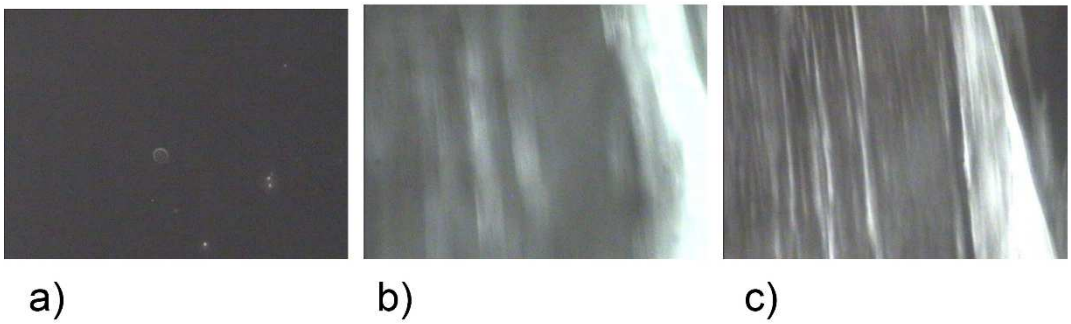

FIGURE 16. *PU2 morphologies at 80°C for a preshear of 40 s^{-1} during 5 s: (a) before preshear, (b) during preshear, and (c) after 3600 s. The height of a picture corresponds to 400 µm.*

CONCLUSIONS

This work was dedicated to the phase separation in TPUs followed by optical and especially rheological means. One of the investigated aspects was the effect of a preshear treatment on this phase separation, which can be linked to the behavior of these materials inside processing tools where they undergo large strain. The first important conclusion, which can be drawn, is that the preshear treatment applied on molten TPU drastically increases the material structuring kinetics. Indeed, for isothermal measurements, the time corresponding to this structuring can be reduced by more than 1 decade. Moreover, the decrease in the structuring time is significant even for very short preshear treatments of a few seconds (to be compared with the structuring time of several hundreds of seconds). In other words, the material exhibits a memory effect of the shear treatment. To our knowledge, this issue was not observed before. Moreover, from the obtained plots for the characteristic solidification times, it can be foreseen that the solidification kinetics is essentially

governed by a thermodynamically controlled process (phase separation and/or crystallization) and not by a diffusional one. Furthermore, this process is largely enhanced by a preshear treatment.

From a morphological point of view, without preshear treatment or with soft shearing conditions, the semicrystalline material (PU1) exhibits a spherulitic structure, whereas no structure is noticeable for the nearly amorphous one (PU2). However, for stronger preshear treatments, both materials practically show the same behavior, namely a global molecular orientation frozen during the shear and evidenced by the birefringent character of the material.

In a more global framework, the continuation of these works could be devoted to different issues. First, the exposed rheological methods could be positively used to scrutinize the influence of the TPU HS nature and length on the temperature dependence of the structuring kinetics by studying a real ''family'' of analogous TPUs with comparable SSs and HSs. Moreover, from a morphological point of view, the preliminary results obtained by optical microscopy should be confirmed using more powerful techniques such as SAXS. Finally, the effect of the morphological anisotropy on the material macroscopic properties (especially mechanical properties) should be investigated.

The authors gratefully acknowledge the Rhône-Alpes region for financial support and the company Nexans for material supply. The authors thank more particularly Olivier Pinto and Jérôme Fournier for stimulating discussions.

REFERENCES AND NOTES

1. Wirpsza, Z. In *Polyurethanes: Chemistry, Technology and Applications*; Kemp, T. J.; Kennedy, J. F.; Mark, J. E., Eds.; Ellis Horwood: Chichester, 1993; pp 95–129.

2. Estes, G. M.; Seymour, R. W.; Cooper, S. L. *Macromolecules* 1971, **4**, 452–457.

3. Petrovic, Z. S.; Ferguson, J. *Prog Polym Sci* 1991, **16**, 695–836.

4. Wang, C. B.; Cooper, S. L. *Macromolecules* 1983, **16**, 775–786.

5. Seymour, R. W.; Cooper, S. L. *J Polym Sci Part B: Polym Lett* 1971, **9**, 689–694.

6. Seymour, R. W.; Cooper, S. L. *Macromolecules* 1973, **6**, 48–53.

7. Leung, L. M.; Koberstein, J. T. *Macromolecules* 1986, **19**, 706–713.

8. Koberstein, J. T.; Russell, T. P. *Macromolecules* 1986, **19**, 714–720.

9. Gibson, P. E.; Bogart, J. W. C. V.; Cooper, S. L. *J Polym Sci Part B: Polym Phys* 1986, **24**, 885–907.

10. Li, Y.; Liu, J.; Yang, H.; Ma, D.; Chu, B. *Polym Mater Sci Eng* 1991, **65**, 297–298.

11. Li, Y.; Gao, T.; Chu, B. *Macromolecules* 1992, **25**, 1737–1742.

12. Chu, B.; Gao, T.; Li, Y.; Wang, J.; Desper, C. R.; Byrne, C. A. *Macromolecules* 1992, **25**, 5724–5729.

13. Li, Y.; Gao, T.; Liu, J.; Linliu, K.; Desper, C. R.; Chu, B. *Macromolecules* 1992, **25**, 7365–7372.

14. Li, Y.; Ren, Z.; Zhao, M.; Yang, H.; Chu, B. *Macromolecule*s 1993, **26**, 612–622.

15. Rangarajan, P.; Register, R. A.; Adamson, D. H.; Fetters, L. J.; Bras, W.; Naylor, S.; Ryan, A. J. *Macromolecules* 1995, **28**, 1422–1428.

16. Quiram, D. J.; Register, R. A.; Marchand, G. R.; Ryan, A. J. *Macromolecules* 1997, **30**, 8338–8343.

17. Yeh, F.; Hsiao, B. S.; Sauer, B. B.; Michel, S.; Siesler, H. W. *Macromolecules* 2003, **36**, 1940–1954.

18. Cooper, S. L.; Tobolsky, A. V. *J Appl Polym Sci* 1966, **10**, 1837–1844.

19. Koberstein, J. T.; Stein, R. S. *J Polym Sci Polym Phys Ed* 1983, **21**, 1439–1472.

20. Koberstein, J. T.; Galambos, A. F.; Leung, L. M. *Macromolecules* 1992, **25**, 6195–6204.

21. Voda, A.; Beck, K.; Schauber, T.; Adler, M.; Dabisch, T.; Bescher, M.; Viol, M.; Demco, D. E.; Blümich, B. *Polym Test* 2006, **25**, 203–213.

22. Chen-Tsai, C. H. Y.; Thomas, E. L.; MacKnight, W. J.; Schneider, N. S. *Polymer* 1986, **27**, 659–666.

23. Qi, H. J.; Boyce, M. C. *Mech Mater* 2005, **37**, 817–839.

24. Nichetti, D.; Grizzuti, N. *Polym Eng Sci* 2004, **44**, 1514–1521.

25. McKierman, R. L.; Heintz, A. M.; Hsu, S. L.; Atkins, E. D. T.; Penelle, J.; Gido, S. P. *Macromolecules* 2002, **35**, 6970–6974.

26. Florez, S.; Munoz, M. E.; Santamaria, A. *J Rheol* 2005, **49**, 313–325.

27. Cossar, S.; Nichetti, D.; Grizzuti, N. *J Rheol* 2004, **48**, 691–703.

28. Yang, W. P.; Macosko, C. W.; Wellinghoff, S. T. *Polymer* 1986, **27**, 1235–1240.

29. Koberstein, J. T.; Gancarz, I.; Clarke, T. C. *J Polym Sci Part B: Polym Phys* 1986, **24**, 2487–2498.

30. Martin, D. J.; Meijs, G. F.; Gunatillake, P. A.; McCarthy, S. J.; Renwick, G. M. *J Appl Polym Sci* 1997, **64**, 803–817.

31. Yamasaki, S.; Nishiguchi, D.; Kojio, K.; Furukawa, M. *Polymer* 2007, **48**, 4793–4803.

32. Grassie, N.; Zulfiqar, M. *J Polym Sci Part A: Polym Chem* 1978, **16**, 1563–1574.

33. Montaudo, G.; Puglisi, C.; Scamporrino, E.; Vitalini, D. *Macromolecules* 1984, **17**, 1605–1614.

34. Camberlin, Y.; Pascault, J. P.; Letoffe´, M.; Claudy, P. *J Polym Sci Polym Chem Ed* 1982, **20**, 1445–1456.

35. Herrera, M.; Matuschek, G.; Kettrup, A. *Polym Degrad Stab* 2002, **78**, 323–331.

36. Lattimer, R. P.; Williams, R. C. *J Anal Appl Pyrolysis* 2002, **63**, 85–104.

37. Lu, Q. W.; Hernandez-Hernandez, M. E.; Macosko, C. W. *Polymer* 2003, **44**, 3309–3318.

38 Assink, R. J Polym Sci Polym Phys Ed 1977, 15, 59–69.

39. Eisenbach, C. D.; Heinemann, T.; Ribbe, A.; Stadler, E. *Angew Makromol Chem* 1992, **202/203**, 221–241.

40. Briber, R. M.; Thomas, E. L. *J Polym Sci Polym Phys Ed* 1985, **23**, 1915–1932.

41. Blackwell, J.; Lee, C. D. *J Polym Sci Polym Phys Ed* 1983, **21**, 2169–2180.

42. Bonart, R.; Morbitzer, L.; Hentze, G. *J Macromol Sci Phys B* 1969, **3**, 337–356.

43. Assink, R. A.; Wilkes, G. L. *Polym Eng Sci* 1977, **17**, 606–612.

44. Wilkes, G. L.; Emerson, J. A. *J Appl Phys* 1976, **47**, 4261–4264.

45. Sung, C. S. P.; Hu, C. B.; Wu, C. S. *Macromolecules* 1980, **13**, 111–116.

46. Naudy, S.; David, L.; Rochas, C.; Fulchiron, R. *Polymer* 2007, **48**, 3273–3285.

47. Koscher, E.; Fulchiron, R. *Polymer* 2002, **43**, 6931–6942.

48. Tribout, C.; Monasse, B.; Haudin, J. M. *Colloid Polym Sci* 1996, **274**, 197–208.

49. Ryan, A. J.; Macosko, C. W.; Bras, W. *Macromolecules* 1992, **25**, 6277–6283.

50. Velankar, S.; Cooper, S. L. *Macromolecules* 1998, **31**, 9181–9192.

51. Yoon, P. J.; Han, C. D. *Macromolecules* 2000, **33**, 2171–2183.

52. Lapprand, A.; Méchin, F.; Pascault, J. P. *J Appl Polym Sci* 2007, **105**, 99–113.

53. Bustos, F.; Cassagnau, P.; Fulchiron, R. *J Polym Sci Part B: Polym Phys* 2006, **44**, 1597–1607.

54. Naudy, S.; Fulchiron, R. *Polym Eng Sci* 2007, **47**, 365–373.

55. Hentschel, T.; Münstedt, H. *Polymer* 2001, **42**, 3195–3203.

56. Lu, G.; Kalyon, D. M.; Yilgör, I.; Yilgör, E. *Polym Eng Sci* 2003, **43**, 1863–1877.

57. Nabeth, B.; Corniglion, I.; Pascault, J. P. *J Polym Sci Part B: Polym Phys* 1996, **34**, 401–417.

58. Dassin, S.; Dumon, M.; Méchin, F.; Pascault, J. P. *Polym Eng Sci* 2002, **42**, 1724–1739.

59. Rek, V.; Govorcin, E. *Adv Sci Technol* 1992, **11**, 173–191.

60. Goveas, J. L.; Milner, S. T. *Macromolecules* 1997, **30**, 2605–2612.

61. Chastek, T. Q.; Lodge, T. P. *Macromolecules* 2004, **37**, 4891–4899.

62. Liu, Z.; Shaw, M.; Hsiao, B. S. *Macromolecules* 2004, **37**, 9880–9888.

63. Lauritzen, J. I.; Hoffman, J. D. *J Appl Phys* 1973, **44**, 4340–4352.

64. Rusinova, E. V. *Polym Sci Ser B* 2006, **48**, 177–186.